Ferromagnetic coupled modes in continuous/granular multilayers: Model and experiments

J. Gómez
Centro Atómico Bariloche and Comisión Nacional de Energía Atómica, 8400 San Carlos de Bariloche, Río Negro, Argentina

J. L. Weston
Center for Materials for Information Technology, Tuscaloosa, Alabama 35487-0209, USA

A. Butera*
Centro Atómico Bariloche and Comisión Nacional de Energía Atómica, 8400 San Carlos de Bariloche, Río Negro, Argentina
(Received 30 May 2007; published 14 November 2007)

We have developed an adapted model in order to describe the ferromagnetic resonance (FMR) spectra in a trilayer system in which two continuous ferromagnetic films are coupled by a granular magnetic spacer. The model allowed us to study the influence that different parameters (e.g., the Fe volume concentration and the thickness of the granular spacer, the exchange coupling field between layers, the microwave frequency, etc.) have on the overall line shape of the spectra. We present the general results predicted by the model and compare them with FMR experimental measurements made on a particular trilayer $\{Fe/[Fe(x)\text{-}SiO_2(1-x)](t)/Ni_{80}Fe_{20}\}$ formed by two continuous ferromagnetic layers, Fe and Permalloy ($Ni_{80}Fe_{20}$), separated by a granular film of Fe-SiO_2, in which we changed the Fe volume concentration x ($0.45<x<0.85$), and the thickness t ($t=1,2,4,9$, and 18 nm) of the granular spacer. Room-temperature FMR measurements were made at the Q ($\nu=34$ GHz) and X bands ($\nu=9.5$ GHz) with the external field applied parallel to the film plane. Two well-resolved absorption modes, one at low fields and another at higher fields, were generally observed. From the dependence of the resonance field and the relative intensity of these modes on x and t it was possible to deduce that the granular layer strongly interacts with the Fe layer, whereas the Permalloy layer is only weakly coupled with the rest of the layers.

DOI: 10.1103/PhysRevB.76.184416 PACS number(s): 75.70.Cn, 76.50.+g, 75.50.Bb

I. INTRODUCTION

The magnetic coupling between two ferromagnetic (FM) films separated by different kinds of spacers has been intensively studied in the last two decades, and new and interesting phenomena have usually been reported. For example, when two magnetic films are spaced by a nonmagnetic metal, an oscillatory change in the sign of the magnetic coupling as a function of the spacer thickness is observed, which has been attributed to a Ruderman-Kittel-Kasuya-Yosida-RKKY-like interaction.[1] Films that are antiferromagnetically coupled also show a very large change in the electrical resistance when a relatively low magnetic field is applied. This effect was called giant magnetoresistance.

Since the discovery of the oscillatory coupling, a lot of different materials have been used as spacers. Among them we can mention insulators,[2] semiconductors,[3] antiferromagnets,[4] or other ferromagnets[5] in which new results were often reported.

Heterogeneous or granular magnetic films consist in a nanostructered system of ferromagnetic particles (for example Fe, Co, Ni, etc.) with a diameter of a few nanometers embedded in an immiscible matrix of SiO_2. Such a system has been widely studied[6] and their magnetic properties, either as a function of the Fe volume concentration x or the film thickness t have been published in the literature.[7]

In this paper we present a phenomenological model which was developed with the aim of explaining the ferromagnetic resonance (FMR) spectrum of a trilayer system in which two FM layers are separated by a granular spacer. The model has been applied to the special case of the trilayer $Fe/[Fe(x)\text{-}SiO_2(1-x)](t)/Ni_{80}Fe_{20}$ in which both x and t of the granular spacer are varied in order to change the magnetic coupling among the different layers.

II. MODEL

The trilayer system to be discussed in this work consists in two continuous ferromagnetic layers separated by a granular spacer of Fe-SiO_2. An exhaustive modeling of this kind of system is very complicated due to the changing magnetic properties of the granular layer with the Fe concentration. Our phenomenological model is based on the experimental fact that, although the FMR line associated with the Fe-SiO_2 is readily observed in single granular films,[7] it could not be observed in these trilayers. This is an indication that there should be some kind of coupling (which we will assume to be direct surface exchange coupling) between the continuous ferromagnetic layer and the Fe-SiO_2 layer. Due to the heterogeneous nature of the spacer, the exchange interaction does not propagate through the Fe-SiO_2 layer in the same manner as it does for a metallic magnetic spacer, but its influence is expected to be more extended than what is normally found for an insulating spacer.

We will describe first the FMR spectra that are usually found when a continuous layer interacts strongly with a granular film. Then we will suppose that each bilayer can be treated as a single equivalent layer, and that these two equivalent layers are coupled by a relatively weak exchange interaction. This picture is sketched in Fig. 1. It is important to mention that the same formalism can be also applied if one of the films does not interact with the spacer. In this case the magnetic properties of the equivalent layer are the same as those of the continuous film.

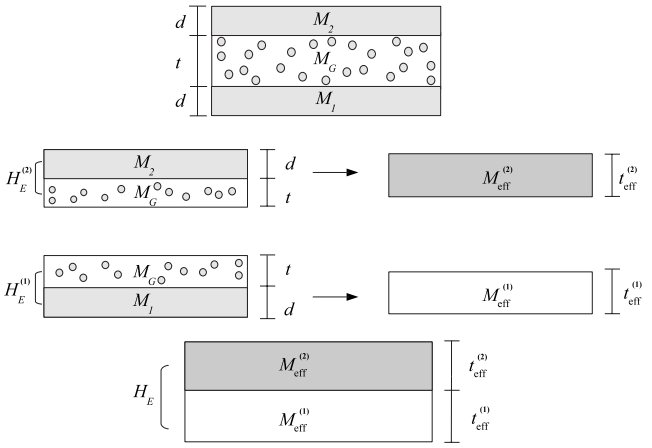

FIG. 1. If we assume that there is a high exchange interaction $H_E^{(i)}$ between the top or bottom continuous layers with the granular spacer, the system can be treated like two separated films M_1/M_G and M_G/M_2. Note that this assumption will be valid only if the Fe concentration of the granular layer is larger that the percolation threshold. The trilayer system can then be modeled as two equivalent layers with effective magnetizations and thicknesses that are coupled by an exchange field H_E.

The problem of two coupled continuous ferromagnetic layers has been treated in detail by several authors.[8,9] When the magnetization of both layers is uniform within the film thickness it is possible to write the magnetic free energy per unit area as

$$F_a = \sum_{i=1}^{2} \left(-d_i \mathbf{M}_i \cdot \mathbf{H} + \frac{d_i}{2} \mathbf{M}_i \underline{\mathbf{N}}_i \mathbf{M}_i + d_i K_n^{(i)} \frac{(\hat{\mathbf{e}}_\perp \cdot \mathbf{M}_i)^2}{|\mathbf{M}_i|^2} \right) - J \frac{\mathbf{M}_1 \cdot \mathbf{M}_2}{|\mathbf{M}_2||\mathbf{M}_1|}. \quad (1)$$

The first term in the above expression is the Zeeman energy, which tends to align the magnetization vectors $\mathbf{M}_i$ in the direction of the external field $\mathbf{H}$, with d_i the film thickness of each layer. The second term corresponds to the demagnetizing energy due to the shape of the film. Because of the large surface to thickness ratio the diagonal demagnetization tensor $\underline{\mathbf{N}}_i$ can be assumed as zero in the film plane and 4π in the perpendicular direction. In the third term we have included an anisotropic contribution which tends to align the magnetization perpendicular to the film. $K_n^{(i)}$ is the perpendicular anisotropy constant and $\hat{\mathbf{e}}_\perp$ is a versor normal to the film plane. The origin of this anisotropy can be the presence of surface tensions, roughness, and any other imperfection which prevents the in-plane alignment of the magnetization. The subscript i indicates that each one of the first three terms in Eq. (1) appears independently for the two magnetic layers. An interlayer coupling of magnitude J (which has units of erg/cm^2) is introduced at the end of Eq. (1) by the bilinear term in the free energy, which favors the alignment of both magnetizations in the same direction. Positive J implies, ferromagnetic coupling. As the experimental data could be reasonably well explained with the magnetic free energy of Eq. (1) there was no need to consider additional energy terms, such as biquadratic exchange or in-plane anisotropy. This assumption limits the number of variables, simplifying the theoretical treatment. In the following analysis the film normal is chosen to be parallel to the y axis; hence $N_{yy}=4\pi$, and the rest of the terms in the demagnetizing tensor are equal to zero.

As reported in Ref. 7, in thin Fe-SiO_2 granular films, the effective value of the magnetization to be used is the average or effective magnetization which is a fraction of the saturation magnetization of Fe. For an ideal heterogeneous sample composed of spherical particles the magnetization should vary as $M_G = xM_{\text{Fe}}$ (M_{Fe} is the saturation magnetization of Fe). This expression proved to be correct especially for $x > x_p$, the magnetic percolation concentration of the metallic granules.[7,10]

The well known Landau-Lifshitz equation of motion can be used to determine the scalar magnetic susceptibility, which gives the overall line shape. From this spectrum it is possible to calculate the resonance field position (maximum in the absorption) and the line intensity (field integral of the absorption).[11] In the present case we have the following equation for each layer:

$$\dot{\mathbf{M}}_i = \gamma \mathbf{M}_i \times \frac{1}{d_i} \frac{\partial F_a}{\partial \mathbf{M}_i} - \frac{\alpha_i}{|\mathbf{M}_i|} \mathbf{M}_i \times \dot{\mathbf{M}}_i - \gamma \mathbf{M}_i \times \mathbf{h}, \quad (2)$$

where $\mathbf{M}_i = \mathbf{M}_{0i} + \mathbf{m}_i e^{i\omega t}$ is the total (radial plus transverse) magnetization of the layer i with $|\mathbf{M}_{0i}| \gg |\mathbf{m}_i|$, $\gamma = g\mu_B/\hbar$ is the gyromagnetic ratio, α_i is the Gilbert damping parameter, and $\mathbf{h}$ is the rf field of frequency ω which is applied normal to $\mathbf{H}$. The g factor value used in granular Fe-SiO_2 is the same as that used for continuous Fe films: $g=2.09$,[7] and for simplicity we have assumed $g=2.09$ for all layers. The two last terms in Eq. (2) are usually neglected if the only variable to be estimated is the field position of the resonance modes.[9] However, when the complete absorption line is needed, all terms in Eq. (2) must be considered. Following Ref. 12 we will express the interlayer magnetic coupling in field units, so that the magnetic exchange field between both layers is given by

$$H_E = J \left(\frac{1}{d_1 |\mathbf{M}_1|} + \frac{1}{d_2 |\mathbf{M}_2|} \right). \quad (3)$$

In the following we will assume $|\mathbf{M}_i| = M_i \simeq |\mathbf{M}_{0i}|$. If the two interacting layers are a continuous film and a granular layer the exchange field becomes

$$H_E^{(i)} = J^{(i)} \left(\frac{1}{d_i M_i} + \frac{1}{t M_G} \right). \quad (4)$$

A. Scalar susceptibility

To obtain an expression for the scalar susceptibility of a coupled bilayer we start introducing explicitly the time dependence $e^{i\omega t}$ in Eq. (2). Keeping terms linear in $\mathbf{m}_i$ and $\mathbf{h}$ and changing the coordinate system to spherical coordinates, it is possible to arrive at the following equation when the external magnetic field is applied parallel to the film plane:

$$\mathbb{D}\mathbf{m} = \tilde{\mathbf{h}}. \tag{5}$$

For this particular case the equilibrium values of the magnetization angles are $\theta_1=\theta_2=\pi/2$, $\varphi_1=\varphi_2=0$. In the above equation, the time-dependent magnetization vector is $\mathbf{m}=(m_{r1},m_{\theta 1},m_{\varphi 1},m_{r2},m_{\theta 2},m_{\varphi 2})$, $\tilde{\mathbf{h}}$ is a linear combination of h_r, h_θ, and h_φ, and the dynamic matrix $\mathbb{D}$ takes the form

$$\mathbb{D} = \begin{pmatrix} i\omega/\gamma M_1 & a & 0 & -c \\ b & i\omega/\gamma M_1 & c & 0 \\ 0 & -d & i\omega/\gamma M_2 & e \\ d & 0 & f & i\omega/\gamma M_2 \end{pmatrix} \tag{6}$$

with

$$a = \frac{1}{M_1}\left(H + 4\pi M_1 - H_n^{(1)} + \frac{J}{d_1 M_1} - \frac{i\alpha_1\omega}{\gamma}\right),$$

$$b = \frac{1}{M_1}\left[\frac{i\alpha_1\omega}{\gamma} - \left(H + \frac{J}{d_1 M_1}\right)\right],$$

$$c = \frac{J}{M_1 M_2 d_1},$$

$$d = \frac{J}{M_1 M_2 d_2},$$

$$e = \frac{1}{M_2}\left(H + 4\pi M_2 - H_n^{(2)} + \frac{J}{d_2 M_2} - \frac{i\alpha_2\omega}{\gamma}\right),$$

$$f = \frac{1}{M_2}\left[\frac{i\alpha_2\omega}{\gamma} - \left(H + \frac{J}{d_2 M_2}\right)\right]. \tag{7}$$

The perpendicular anisotropy fields are defined through $H_n^{(i)}=2K_n^{(i)}/M_i$. Note that $\mathbb{D}$ is a 4×4 matrix because we have omitted the radial terms m_{r1}, m_{r2}, and h_r, which do not contribute to the dynamic behavior of the problem. From the expressions above, it is easily observed that when $J=0$ the dynamic matrix becomes the same as what is expected for two uncoupled films ($c=d=0$).

Equation (5) can be inverted so as to express the transverse magnetization as a function of the excitation rf field,

$$\mathbf{m} = \mathbb{D}^{-1}\mathbb{C}\mathbb{C}^{-1}\tilde{\mathbf{h}} = \underline{\chi}\mathbf{h}. \tag{8}$$

The matrix $\mathbb{C}$ is a change of basis matrix that converts $\tilde{\mathbf{h}}$ to $\mathbf{h}=(h_\theta,h_\varphi,h_\theta,h_\varphi)$ and hence the expression for the magnetic susceptibility tensor is given by $\underline{\chi}=\mathbb{D}^{-1}\mathbb{C}$. This expression is normally too large and complicated, and numerical calculation is generally required to study the resonance line shape in different conditions. The absorption intensity measured in an electron spin resonance (ESR) experiment is proportional to the field integral of the imaginary part of the scalar susceptibility χ,[11] which has the following expression:

$$\chi = \chi' + i\chi'' = \frac{1}{h^2}\mathbf{h}^\dagger\underline{\chi}\mathbf{h}. \tag{9}$$

In the present analysis the absorption line shape is normally formed by two Lorentzian lines. The expression of χ'' can then be used to study the influence that different parameters have on the resonance field and the intensity of the lines that appear in the spectra, as well as to observe the contribution that each layer has on the absorption modes.

B. Highly coupled continuous/granular layers

When the exchange field $H_E^{(i)}$ between the continuous layer i and the granular spacer is much larger than the rest of the fields involved in the problem, both films must respond to the external magnetic field like a single entity because the exchange interaction strongly couples the magnetization of each layer. We have calculated the dispersion relation for the case of very large $H_E^{(i)}$ ($H_E^{(i)} \gg \omega/\gamma$) and H applied in the film plane to obtain

$$\left(\frac{\omega}{\gamma}\right)^2 = H(H + H_{\text{eff}}^{(i)}), \tag{10}$$

with

$$H_{\text{eff}}^{(i)} = 4\pi\left(\frac{d_i M_i^2 + tM_G^2}{d_i M_i + tM_G}\right). \tag{11}$$

The subscript i refers to the continuous layer 1 or 2, and t and M_G are the thickness and the magnetization of the granular layer.

We can compare the result of Eq. (10) with $(\omega/\gamma)^2 = H(H+4\pi M)$, the dispersion relation obtained for a single ferromagnetic film with a saturation magnetization equal to M. In this way we can model two layers with a very large exchange interaction like a single layer having an effective magnetization M_{eff} of magnitude

$$M_{\text{eff}}^{(i)} = \frac{d_i M_i^2 + tM_G^2}{d_i M_i + tM_G} \tag{12}$$

and an effective thickness t_{eff}

$$t_{\text{eff}}^{(i)} = \frac{(d_i M_i + tM_G)^2}{d_i M_i^2 + tM_G^2}. \tag{13}$$

The effective thickness $t_{\text{eff}}^{(i)}$ is derived in such a way that it conserves the total magnetization per unit area ($t_{\text{eff}}^{(i)} M_{\text{eff}}^{(i)} = d_i M_i + tM_G$) or, in other words, it conserves the intensity of the FMR spectra when describing the real bilayer as an equivalent system.

In the next sections of this paper we will treat the real system FM(1)/granular/FM(2) like an equivalent bilayer with different effective magnetizations $M_{\text{eff}}^{(1)}$ and $M_{\text{eff}}^{(2)}$ in which the interlayer interaction is relatively weak, as already depicted in Fig. 1. We will then use Eqs. (1) and (2) to describe the equivalent bilayer system, introducing an exchange field H_E and calculating the scalar susceptibility [Eq. (9)] in order to study the relative intensities and the field position of the resonance modes.

C. Resonance field positions in the equivalent bilayer system

We can evaluate Eqs. (12) and (13) using the magnetization values corresponding to each layer: $M_1=M_{\text{Fe}}$

TABLE I. Values of M_{eff} and t_{eff} obtained from Eqs. (12) and (13) for the equivalent bilayer system. d and t are the thicknesses of the top (and bottom) layer and the granular spacer, respectively.

	M_{eff}	t_{eff}
(1) Fe(d)/Fe-SiO_2(t)	$M_{\text{Fe}}\frac{d+tx^2}{d+tx}$	$\frac{(d+tx)^2}{d+tx^2}$
(2) Fe-SiO_2(t)/Py(d)	$\frac{dM_{\text{Py}}^2+t(xM_{\text{Fe}})^2}{dM_{\text{Py}}+txM_{\text{Fe}}}$	$\frac{(dM_{\text{Py}}+txM_{\text{Fe}})^2}{dM_{\text{Py}}^2+t(xM_{\text{Fe}})^2}$

~ 1700 emu/cm^3, $M_G=xM_{\text{Fe}}$, and $M_2=M_{\text{Py}}=816$ emu/cm^3 (Py refers to $Ni_{80}Fe_{20}$). The corresponding expressions are shown in Table I. These expressions have an explicit dependence on the spacer thickness t and the Fe volume concentration x of the granular layer. These two parameters will then determine the overall behavior of the FMR spectra.

It is important to note that, when the Fe concentration in the granular spacer is low ($x<x_p$), the magnetic interaction among grains decreases, and the interaction with the continuous layer is considerably suppressed. Also, if the spacer thickness t is too large, the continuous layer cannot interact efficiently with the whole granular spacer. The present model should be applied with care in these two limits.

1. Zero exchange interaction

In the case $H_E\sim 0$ we expect to have two absorption signals, one resonating at a field H_{r1}, which corresponds to the resonance of the equivalent system with effective magnetization $M_{\text{eff}}^{(1)}$, and another at a field H_{r2} associated with $M_{\text{eff}}^{(2)}$. In Fig. 2 we show the dependence of the resonance field position of the uncoupled equivalent system ($H_E=0$) on the external magnetic field applied parallel to the film plane as a function of t for different values of x. Data have been simulated for the Q-band frequency ($\nu=34$ GHz).

The main feature that can be observed in Fig. 2 is that the position of the resonance fields is shifted as x or t are varied. In particular, H_{r1} increases for larger t and the opposite trend occurs for H_{r2} in this range of x. For a fixed thickness both resonance fields move to lower values when x increases. The origin of this behavior resides in the different magnetization values of the three layers ($M_{\text{Fe}}>xM_{\text{Fe}}>M_{\text{Py}}$). Due to this difference and the dependence of M_{eff} on the Fe concentration of the granular layer, the effect of the granular spacer is to increase the resonance field of the Fe-like equivalent layer and to lower the field of the $Ni_{80}Fe_{20}$-like film when $x>M_{\text{Py}}/M_{\text{Fe}}$. As it is seen in Fig. 2, the shift of the resonance field is much more evident in H_{r2}, especially for large values of x and t.

It is also of interest to analyze the dependence of the resonance field as a function of the thickness of the spacer for different excitation frequencies. In Fig. 3 we show the dispersion relation, Eq. (10), as a function of t ($t=1,2,4,9$, and 18 nm) for a fixed concentration ($x=0.59$) and for the Fe/Fe-SiO_2 equivalent layer with $M=M_{\text{eff}}^{(1)}$. The horizontal lines represent the X- and Q-band excitation frequencies. The position of the resonance field H_{r1} is shifted to higher fields for larger values of t at all frequencies, but this variation is much more noticeable in Q-band measurements as indicated by the vertical lines in Fig. 3. A similar behavior was also observed in Ref. 13 in symmetric trilayers. The shift in this resonance field is also affected by the value of x and is larger when x takes smaller values.

2. Magnetic coupling between $M_{eff}^{(1)}$ and $M_{eff}^{(2)}$

After the values of $M_{\text{eff}}^{(1)}$, $M_{\text{eff}}^{(2)}$, and the other parameters involved in Eq. (2) are determined, the effect of H_E on the resonance modes can be explored. The scalar susceptibility calculated from Eq. (9) is then used to study the influence of the exchange field H_E on the absorption spectra.

For positive H_E (ferromagnetic coupling) the main changes that can be found are the shift in the position of both resonance fields to lower values, and the decrease in the

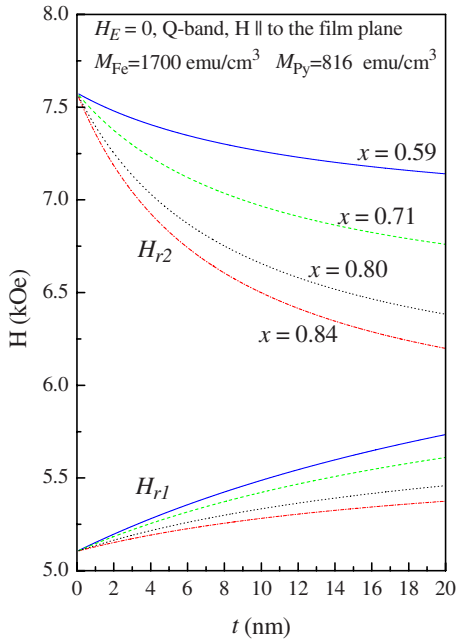

FIG. 2. (Color online) Predicted values of the resonance fields H_{r1} and H_{r2} as a function of t for different values of x for the uncoupled equivalent system in the case $H_E=0$. Simulations have been made for the Q band and with the external field applied in the film plane. Labels for the x variable also apply to the lower set of curves.

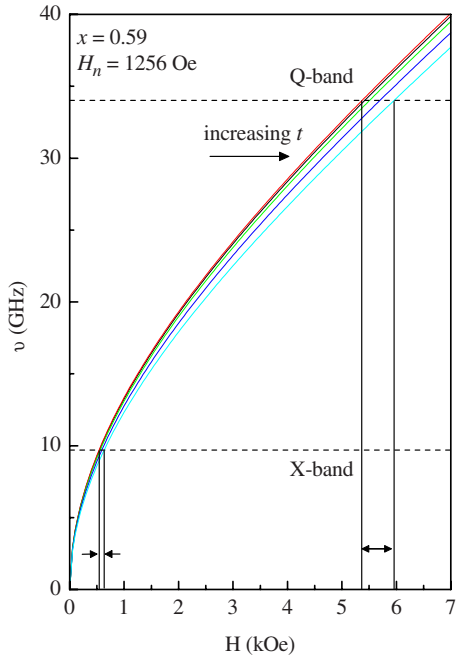

FIG. 3. (Color online) Dispersion relation for the mode associated with the layer with effective magnetization $M_{\text{eff}}^{(1)}$. Values of the spacer thickness are $t=1,2,4,9$, and 18 nm. The concentration $x=0.59$ was kept constant. Dashed horizontal lines correspond to 9.5 and 34 GHz frequencies. The vertical lines indicate the shift of the resonant field at these two frequencies.

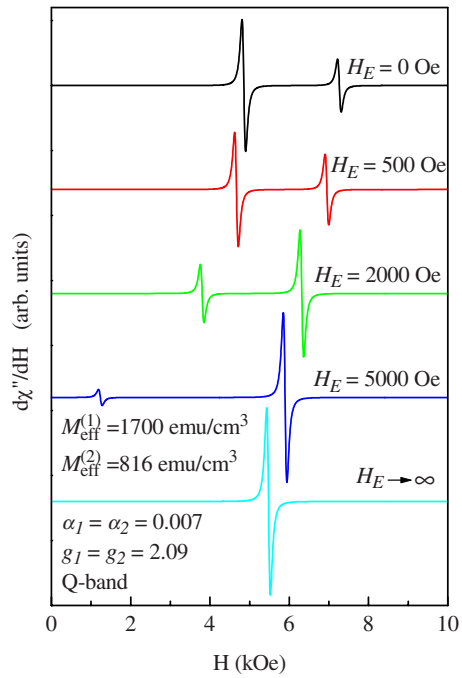

FIG. 4. (Color online) FMR spectra simulations for different values of the exchange coupling field H_E. The external field is applied in the film plane. Note that for very large values of H_E only one line can be detected.

relative intensity ratio I_1/I_2, where I_1 and I_2 are the intensities of modes 1 and 2, respectively.

Figure 4 shows a set of curves in which the exchange field H_E is increased from zero to larger values, as indicated in the figure. If we assume that the anisotropy and exchange fields are small enough (i.e., smaller than the microwave excitation frequency in field units), the frequency gap in the dispersion relation will be small and the total intensity of the spectrum should change very little when H_E is varied. In this case (I_1+I_2) must be almost constant, but the intensity of each mode can change considerably. When $H_E>0$ the mode corresponding to H_{r1} moves to lower fields and decreases its intensity while I_2 increases accordingly in order to maintain the total intensity. When the exchange field is much larger than the measurement frequency, the low-field mode is no longer observed and the strongly coupled bilayer behaves again like a unique entity with an intensity proportional to the total number of moments present in the system. In Sec. II B we have assumed that this situation happens between the continuous and the granular layers in order to treat the coupled bilayer as an equivalent single layer.

The variation of the relative intensity ratio between the two modes is a parameter that could be used to estimate H_E from the experimental measurements even when the values of H_E are small. This is especially useful when the resonance fields could not be accurately determined, for example if a small in-plane uniaxial anisotropy is present.

Although in a real spectrum one observes the response of the whole system, in Eqs. (8) and (9) it is possible to separate the individual contribution of the two layers to the FMR line. In this way we can investigate the effect that the exchange constant has on each subsystem. The contribution of each layer in the case of noninteracting layers ($H_E=0$) is shown in Fig. 5(a). In this case the out of diagonal block terms in the dynamical matrix $\mathbb{D}$ are zero and the total spectrum is simply composed by the addition of the individual resonances of each layer. In Fig. 5(b) the case in which $H_E>0$ is depicted. In this condition both layers contribute to each mode because the out of diagonal terms are not zero. Note that while $M_{\text{eff}}^{(1)}$ has an in-phase contribution to the intensity of the line resonating at H_{r2}, the contribution of $M_{\text{eff}}^{(2)}$ to H_{r1} has a phase shift of 180°. This is the reason why the intensity of the low-field mode decreases (and the intensity of the line at H_{r2} increases) when H_E increases. Of course in a real experiment the counterphase line is not observed. What happens is that, when $M_{\text{eff}}^{(1)}$ and $M_{\text{eff}}^{(2)}$ precess with a phase shift of 180°, the total transversal magnetization parallel to the rf field is smaller, and for this reason the intensity of the line resonating at H_{r1} decreases.

III. COMPARISON WITH EXPERIMENTAL DATA

A preliminary experimental study of Fe/Fe-SiO_2/Py trilayers was recently reported in Ref. 14. In order to compare the present model with the experimental results we have extended those measurements to *X*-band frequencies (9.5 GHz) and have analyzed a larger number of samples. The trilayers were grown using the same method described in Refs. 13 and 14. Briefly, the continuous FM layers were dc sputtered from either an Fe or a $Ni_{80}Fe_{20}$ target and the

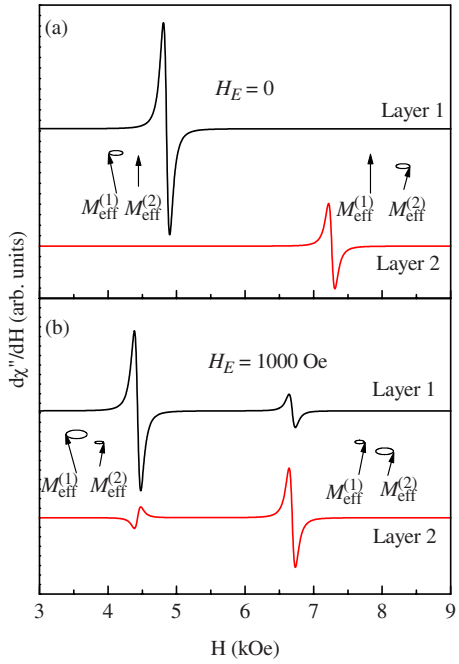

FIG. 5. (Color online) Contribution of each layer to the FMR spectra in the uncoupled (a) and coupled (b) cases. The resultant line is formed by the addition of the two spectra. The same parameters as in Fig. 4 have been used.

granular spacer layer was grown using rf sputtering from a SiO_2 target whose upper half was covered with an Fe foil. The Fe continuous film was deposited first, followed by the granular and the Permalloy layers. Due to the limited number of magnetron sputtering guns in the chamber it was necessary to break down the vacuum after growing the granular film. A top SiO_2 layer was finally deposited to prevent oxidation of the system. The thickness of the two continuous FM layers was kept fixed at $d=17$ nm. Five sets of samples with a different spacer thickness t ($A=1$ nm, $B=2$ nm, $C=4$ nm, $D=9$ nm, and $E=18$ nm) were fabricated. In each series the Fe volume concentration of the granular layer was in the range $0.45 \leq x \leq 0.85$.

FMR measurements have been done with a commercial Bruker ESP 300 spectrometer operating at either X or Q band.

A. Results and discussion

The experimental FMR measurements show two absorption signals in all the studied samples, at both Q and X bands. The resonance field of each signal was found close to the positions expected for single continuous Fe (H_{r1}) and $Ni_{80}Fe_{20}$ (H_{r2}) films, respectively. We have not observed any other signal that could be associated to the magnetic response of the granular spacer. This signal is readily observed in single heterogeneous films,[7] so that its absence in the trilayers is suggesting that there could be an exchange interaction between the granular layer and the continuous films. Although the FMR signal of the spacer is not observed, the discussion in the previous sections indicates that the presence of the granular layer should affect the position and the intensity of the other two lines.

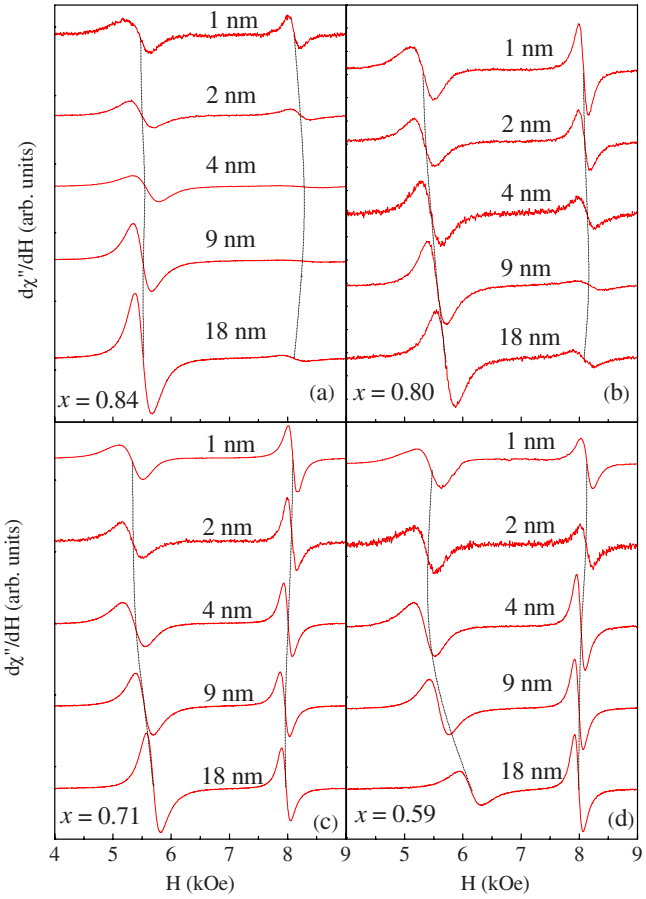

FIG. 6. (Color online) Experimental FMR spectra from different samples taken at the Q band and normalized by the intensity of the absorption at higher fields. Dashed lines indicate the position of the resonance field.

FMR measurements of different samples (made with the external magnetic field applied parallel to the film plane) are shown in Fig. 6. We present four set of curves, each set having five spectra with the same x value but different spacer thickness. When each continuous layer is strongly coupled with the granular spacer the variation of the resonance field must behave as is shown in Fig. 2. The experimental results indicate that only the Fe-like absorption mode shifts to higher fields and that the resonance field associated with the $Ni_{80}Fe_{20}$ layer remains almost unaffected. This is suggesting that there is a very weak interaction between the Permalloy film and the rest of the layers. The origin of this behavior is probably due to the need to break down the vacuum in the fabrication process, allowing the formation of a thin oxide layer which hinders the magnetic interaction between the $Ni_{80}Fe_{20}$ and the granular layer.

The discussion in the above paragraph suggests that the Fe and Fe-SiO_2 layers are highly exchange coupled and they could be treated like an effective unique layer that interacts only weakly with the $Ni_{80}Fe_{20}$ film. Under this hypothesis, the corresponding value for the effective magnetizations are $M_{\rm eff}^{(1)} = M_{\rm Fe}[(d+tx^2)/(d+tx)]$, $M_{\rm eff}^{(2)} = M_{\rm Py}$.

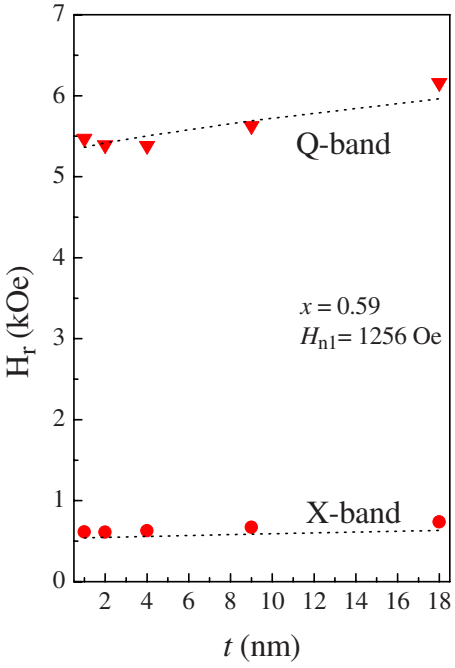

FIG. 7. (Color online) Resonance field position H_{r1} as a function of t for different rf frequencies and x=0.59. Dashed lines correspond to the fit obtained from the proposed model.

Neglecting the presence of a small in-plane uniaxial anisotropy, the field position of the resonance mode H_{r1} can be obtained from the dispersion relation derived from the analysis of Sec. II:

$$\left(\frac{\omega}{\gamma}\right)^2 = H_{r1}\left(H_{r1} + 4\pi M_{\mathrm{Fe}}\frac{d+tx^2}{d+tx} - H_{n1}\right), \qquad (14)$$

where we have defined H_{n1} as the perpendicular anisotropy field of the effective layer (1).

Figure 6 also shows that H_{r2} stays almost constant, suggesting that the interaction of the Fe/Fe-SiO_2 bilayer with the $Ni_{80}Fe_{20}$ layer is very weak. As predicted by the model, a large exchange field should give a considerable shift of the resonance field of the Py layer, larger in general than that produced in the Fe/Fe-SiO_2 equivalent layer (see Fig. 2).

As already mentioned, the shift in the position of the resonance field depends on the excitation frequency (see Fig. 3). In general, the dispersion relation changes in such a way that the variations of the resonance field are more noticeable for higher rf frequencies. In Fig. 7 we show the dependence of the in-plane resonance field H_{r1} when varying t for a fixed spacer concentration x, at both Q and X bands. Using Eq. (14), we have fitted the experimental FMR resonance field H_{r1} measured at two different frequencies. The agreement between data and model is quite good, taking into account that the only free parameter in Eq. (14) is the out-of-plane anisotropy field H_{n1}, and that the same value of H_{n1} was used for all the samples. Note that, as the thickness of the bottom Fe layer has been kept fixed, the fact that the value of the perpendicular anisotropy is similar in all films suggests that the contribution of the granular layer to H_{n1} is very small.

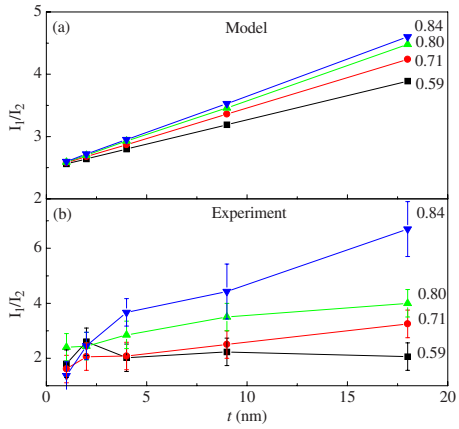

FIG. 8. (Color online) (a) Variation of the relative line intensity I_1/I_2 as a function of t for different values of x in the case H_E=0 deduced from the proposed model. (b) Experimental values of I_1/I_2 obtained from the spectra of Fig. 6.

From the proposed model it is also possible to compare the relative intensity ratio (I_1/I_2) with the experimental data. As the thickness d of the Fe and Permalloy layers does not change in different samples, their contribution to the absorption intensity of H_{r1} and H_{r2} should be approximately the same in all cases. Considering that the granular spacer interacts mostly with the Fe layer it must mainly contribute to the intensity of the H_{r1} mode so that the intensity ratio (I_1/I_2) must increase for higher values of t. The experimental measurements reflect this situation as can be seen in Fig. 6, especially in the two upper panels. For lower values of x a careful determination of the intensity also verifies these predictions.

In Fig. 8(a) we show the behavior of the relative intensity I_1/I_2 when t and x are varied, in the case H_E=0. This figure can be compared directly with the intensity values obtained from Fig. 6 which are shown in Fig. 8(b). Although some uncertainty exists in the determination of these values, it can be seen that the increase of intensity with the thickness and the Fe concentration of the granular layer are in reasonably good agreement with the predictions of the model.

Discrepancies between the model and the experimental intensity ratio can be better accounted for if an exchange interaction between both layers is included. The effect that a nonzero H_E between the magnetization $M_{\mathrm{eff}}^{(1)}$ of the Fe/Fe-SiO_2 coupled layer and the magnetization of the $Ni_{80}Fe_{20}$ layer has on the absorption spectra is to change the resonance field positions H_{r1} and H_{r2} and to modify the relative intensity ratio I_1/I_2. The effect generated by the increase of H_E has been already shown in Figs. 4 and 5. In the samples that we are using to compare with our model, the exchange coupling is relatively small, probably because of the need to break down the vacuum in the fabrication process allowing the presence of a thin oxide layer, which hinders the interaction between the Permalloy and the granular layer. The small values of H_E and the presence of a small in-plane uniaxial anisotropy complicates the estimation of the ex-

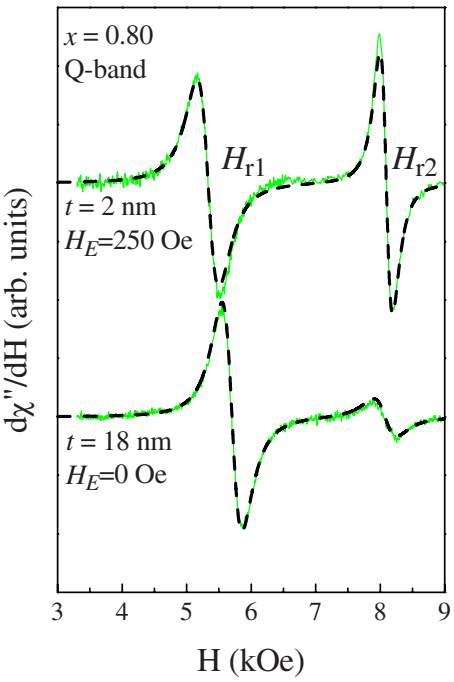

FIG. 9. (Color online) FMR spectra for the samples with $x=0.80$, $t=2$ nm and $x=0.80$, $t=18$ nm. Continuous lines correspond to the experimental data and the dashed lines correspond to the fit with the following parameters. Top spectra: $M_{\text{eff}}^{(1)}=1670$ emu/cm^3, $t_{\text{eff}}^{(1)}=18.92$ nm, $M_{\text{eff}}^{(2)}=816$ emu/cm^3, $\alpha_1=0.026$, $\alpha_2=0.015$, $H_E=250$ Oe, $H_{n1}=2890$ Oe, $H_{n2}=3116$ Oe. Bottom spectra: $M_{\text{eff}}^{(1)}=1542$ emu/cm^3, $t_{\text{eff}}^{(1)}=34.56$ nm, $M_{\text{eff}}^{(2)}=816$ emu/cm^3, $\alpha_1=0.024$, $\alpha_2=0.0275$, $H_E=0$, $H_{n1}=2764$ Oe, $H_{n2}=2576$ Oe.

change coupling field using only the shifts of the resonance fields. As we have mentioned before it is expected that H_E increases when t decreases or when x increases, because the influence of the Fe/Fe-SiO_2 equivalent layer over $Ni_{80}Fe_{20}$ will be more notorious.

The effects of H_E on the spectra intensity are shown in Fig. 9 for two samples with different spacer thickness ($t=2$ and 18 nm) and with $x=0.8$. It is observed that for small spacer thicknesses an exchange field of $H_E \sim 250$ Oe must be included in order to correctly reproduce the intensity ratio. When the spacer is thicker the interaction almost disappears and the spectrum could be well fitted assuming no exchange field between the layers. We would like to emphasize that, even though the precise determination of H_E is affected by different factors, the overall line shape was very well reproduced using a relatively small set of parameters.

IV. CONCLUSION

We have developed a model to describe the resonance spectra of trilayers composed by continuous ferromagnetic films separated by a granular magnetic spacer. We have found a series of properties predicted by the model, and these predictions were compared with FMR measurements made in a series of samples in which both the spacer thickness and the concentration of the magnetic grains were varied. Changes in the position of the resonance field and the line intensity as a function of x and t are well described by our model, at both at Q- and X-band frequencies. For the particular samples used to test our model, the influence of the exchange field between layers H_E is too small to show a systematic change in H_E as a function of t or x. However, it was still possible to obtain a very good fit of the FMR spectra of the samples and, as expected, the larger values of H_E occur for the thinner and more concentrated spacers.

ACKNOWLEDGMENTS

We wish to acknowledge the support of ANPCyT, Argentina, through Grant No. PICT 03-13297; Conicet, Argentina through Grant No. PIP 5250; and U. N. Cuyo through Grant No. 680/05.

*Also at Consejo Nacional de Investigaciones Científicas y Técnicas, and Instituto Balseiro, Universidad Nacional de Cuyo, Argentina. butera@cab.cnea.gov.ar

[1] S. S. P Parkin, R. Bhadra, and K. P Roche, Phys. Rev. Lett. **66**, 2152 (1991)

[2] C. L. Platt, M. R. McCartney, F. T. Parker, and A. E. Berkowitz, Phys. Rev. B **61**, 9633 (2000).

[3] G. J. Strijkers, J. T. Kohlhepp, H. J. M. Swagten, and W. J. M. de Jonge, Phys. Rev. Lett. **84**, 1812 (2000).

[4] H. Xi and R. M. White, Phys. Rev. B **62**, 3933 (2000).

[5] A. Butera, J. L. Weston, and J. A. Barnard, IEEE Trans. Magn. **38**, 2862 (2002).

[6] J. N. Zhou, A. Butera, H. Jiang, and J. A. Barnard, J. Appl. Phys. **84**, 5693 (1998); J. N. Zhou, A. Butera, H. Jiang, D. H. Yang, and J. A. Barnard, *ibid.* **85**, 6151 (1999).

[7] A. Butera, J. N. Zhou, and J. A. Barnard, Phys. Rev. B **60**, 12270 (1999); J. Gómez, A. Butera, and J. A. Barnard, *ibid.* **70**, 054428 (2004); G. N. Kakazei, A. F. Kravets, N. A. Lesnik, M. M. Pereira de Azevedo, Yu. G. Pogorelov, and J. B. Sousa, J. Appl. Phys. **85**, 5654 (1999).

[8] B. Heinrich, S. T. Purcell, J. R. Dutcher, K. B. Urquhart, J. F. Cochran, and A. S. Arrott, Phys. Rev. B **38**, 12879 (1988).

[9] A. Layadi and J. O. Artman, J. Magn. Magn. Mater. **92**, 143 (1990).

[10] N. A. Lesnik, C. J. Oates, G. M. Smith, P. C. Riedi, G. N. Kakazei, A. F. Kravets, and P. E. Wigen, J. Appl. Phys. **94**, 6631 (2003).

[11] U. Netzelmann, J. Appl. Phys. **68**, 1800 (1990). A. Butera, Eur. Phys. J. B **52**, 297 (2006).

[12] Z. Zhang, L. Zhou, P. E. Wigen, and K. Ounadjela, Phys. Rev. B **50**, 6094 (1994).

[13] J. Gómez, J. L. Weston, and A. Butera, J. Appl. Phys. **100**, 053908 (2006).

[14] J. Gómez, A. Butera, and J. L. Weston, Physica B **384**, 277 (2006).